Proceedings of the Institution of Mechanical Engineers, Part B: Journal of Engineering Manufacture
http://pib.sagepub.com/

Field feature detection and morphing-based process planning for fabrication of geometries and composition control for functionally graded materials

R Dwivedi, S Zekovic and R Kovacevic

Proceedings of the Institution of Mechanical Engineers, Part B: Journal of Engineering Manufacture 2006 220: 1647
DOI: 10.1243/09544054JEM490

Field feature detection and morphing-based process planning for fabrication of geometries and composition control for functionally graded materials

R Dwivedi, S Zekovic, and **R Kovacevic***
Research Center for Advanced Manufacturing, Southern Methodist University, Richardson, Texas, USA

The manuscript was received on 27 October 2005 and was accepted after revision for publication on 31 May 2006.

DOI: 10.1243/09544054JEM490

Abstract: The inherent limitation of most solid freeform fabrication (SFF) is deposition in the form of layers. The set-up rather than the geometry and the material composition of the part becomes more important in the process planning. For a functionally graded material (FGM), the desired composition variation is of infinitesimal order; however, the finite size of the deposition head and the molten pool allows for a quantized volume addition. Such artificial imposition of the process for the desired geometric morphology and the functional gradience of materials limit the accuracy of the part. The frequent variation in the material composition is yet another issue associated with the fabrication of FGMs. The suitability of a field can be attributed to the desired material distribution of a part. Different features of the field are identified and used as the input for process planning. The mathematical morphing of the material gradience allows a smooth variation of the material composition across the geometry of the part during deposition. The paper describes a framework for FGM representation using maxel, process planning, and implementation of the fabrication of geometries, and the control of the material composition. The experimental results for the suggested approach are described.

Keywords: solid freeform fabrication, functionally graded material, maxel, isocomposition contours, multimaterial solid

1 INTRODUCTION

Of the various features associated with solid freeform fabrication (SFF), what makes it unique is the ability to control material composition and fabricate hidden geometric features. In SFF, deposition of the material takes place in the form of layers. Layered addition of material allows process planning to be independent of part morphology. The path for the material deposition head along each layer is based on the distribution of two-dimensional curves. For a major class of parts fabricated by SFF, layered deposition and the subsequent independence of the process with respect to the part morphology is acceptable. Most of the deposition processes are based on the delivery of material in a discrete amount, which limits the accuracy of the geometry. The post-processing such as machining is done in order to remove unwanted material and obtain a precise geometry. Material composition on the other hand must be controlled very precisely during addition because it is not possible to alter the material composition once the material has been deposited. Recent developments in technology such as computer-based geometry representation and the very precise control of electric drives have allowed the fabrication of a variety of functionally graded material (FGM). An FGM part may be characterized by the variation in composition and structure gradually over volume, resulting in corresponding changes in the properties of the material. Materials can be designed for a specific function and specific applications. Various approaches based on the bulk (particulate processing), preform processing, layer

**Corresponding author: Department of Mechanical Engineering, Southern Methodist University, Research Center for Advanced Manufacturing, 1500 International Parkway, Suite no. 100, Richardson TX 75081, USA. email: kovacevi@engr.smu.edu*

processing and melt processing are used to fabricate FGMs [**1**]. SFF, owing to its inherent capability of accessing all the points in part geometry, has become a popular method for the fabrication of FGMs.

Any FGM implementation system consists of four fundamental units:

(a) material feeder;
(b) mixer;
(c) spatial manipulator;
(d) deposition head.

The material feeder feeds different materials in the desired composition. The mixer prepares a uniform blend of individual components, and the spatial manipulator delivers the material at a desired location. Direct laser metal deposition is one of the popular methods for metal deposition for SFF, especially for the fabrication of FGM parts. It comprises the system used to implement metal deposition using laser-based direct metal deposition (LBDMD). In the LBDMD, a molten pool is formed on a metallic substrate by focusing a laser; then build metal is delivered directly to the molten pool via a powder delivery system. The use of suitable hardware and software allows real-time adjustments to the mixture of metal powder entering the molten pool, and hence the deposited material's composition [**2**]. For the fabrication of the FGM, powdered metal is fed from the respective powder feeders in a suitable proportion. An inert gas such as argon serves as the carrier medium for the metal powder. Metal powders from different powder feeders are mixed to generate a single mixture which is delivered to the molten pool. In order to achieve the desired uniform composition of alloy, the stream of powders must flow through a mixing mechanism over a suitable interval of time. In the LBDMD, turbulence in carrier gas allows free mixing of the powders. However, the flow must take place over a suitable length of conduit in order to obtain a uniform desired composition.

For FGM parts, the fabrication set-up limits the accuracy of the desired composition of the part owing to frequent variation in the composition of material. This imposes a requirement for suitable process planning that minimizes the variation in the composition of the material being added during the material addition process. Issues inherent in achieving the desired composition include a time lag between asking for a given composition and when the composition is actually injected into the molten pool [**3**]. The most significant parameters that affect the timings include the geometry of the tubing used to carry powder from the feeder to the deposition head [**3**] and the speed of the powder stream. Conversely, when the composition of metal powders is changed, pre-existing material in the conduits must be removed. The method outlined in this paper optimizes the powder delivery so as to minimize the frequency of variation in metal composition during the delivery. The process planning approach also describes an analytical model for the determination of time for discharge of unwanted material when the laser deposition head moves from one region to another. It also suggests an approach for determining the time before the flow of material and subsequent composition becomes uniform.

The method suggested in this paper optimizes powder delivery so as to minimize the frequency of variation in the metal composition during delivery, and also suggests an analytical model for determining the time for the discharge of unwanted material when the metal deposition head moves from one region to another and the time before the flow of the material and the subsequent composition becomes uniform.

Section 1 of the paper identifies a list of parameters for the desired accuracy of the part geometry and a material composition. Section 2 discusses the different methods used to represent FGM parts. Section 3 discusses the mathematical basis of the process and a suitable derivation of the process model. Section 4 elaborates on different approaches of path planning and the selection of the path-planning approach for metal deposition. Lastly, the actual process implementation, simulation, and experimental results are described.

2 IDENTIFICATION OF TASKS ASSOCIATED WITH THE FABRICATION OF FUNCTIONALLY GRADED MATERIAL PARTS

The fabrication of FGMs can be divided into two subtasks: firstly, the fabrication of the geometry; secondly, the control of the delivery of the material composition at a given location. The desired geometry of a part, fabricated by SFF, is obtained by the relative motion of the substrate and metal deposition head. Essentially, the relative motion is implemented by the control of the input signals for the electric drives that control the x, y, and z motions and the relative orientation of the substrate (Fig. 1). Similarly, the control of the part composition is based on the control of electric drives that control the delivery of volume of the constituents. The two subtasks are, however, not independent and therefore require a comprehensive control approach. The basic aim of process planning is to transform the computer model of the part to one that is suitable for implementation using a machine. The input into the process planning system is a computer model of the part; therefore, the method of representation of the part becomes an essential factor.

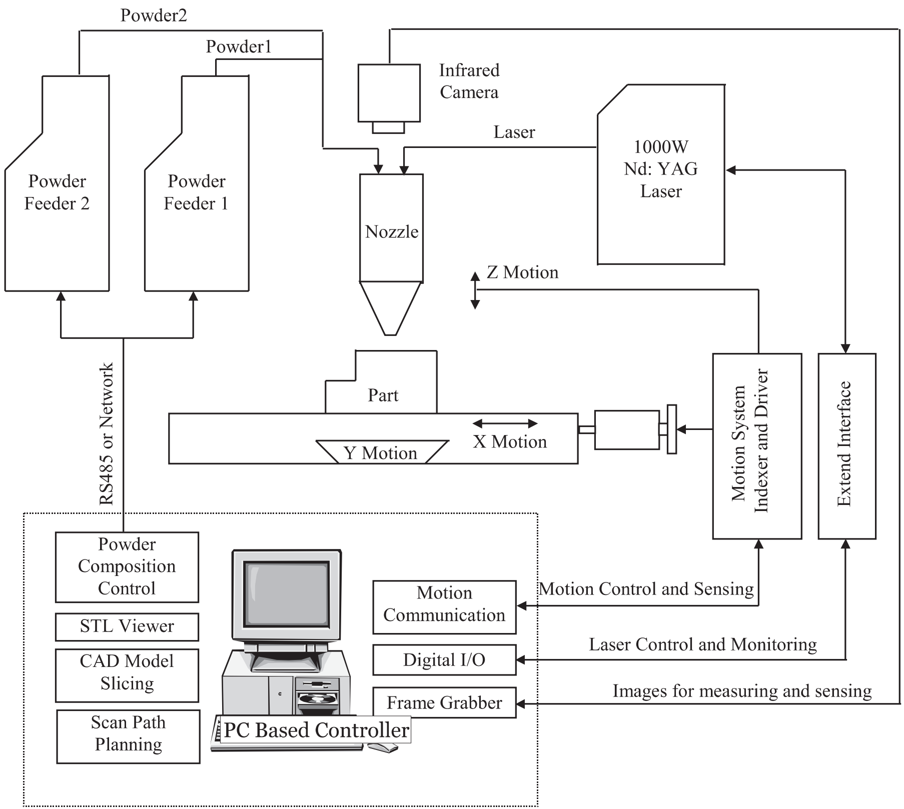

Fig. 1 System for FGM fabrication using laser-based direct metal deposition

Approaches for representation of FGM parts in the recent literature [**4–16**] include the decomposition-based method, the B-rep method, the extended cell-tuple structure-based method and the distance field method. The decomposition-based method subdivides the space into multiple subregions and associates the material information with the subregions [**4**]. The B-rep method is based on describing the solids in terms of bounding topological entities followed by the finite subdivision of the solid into material domains and associating a material variation function over the domain [**5**, **10**]. In the extended cell-tuple structure-based method, a model is represented by a set of topological entities such as vertex-, edge-, face-, and region-called cells that are connected through a graph, and the composition information is associated with each cell [**6**]. The central notion of the use of the distance field is based on the parameterization of space by the distance from the material features, either exactly or approximately [**7**]. While the multimaterial solids essentially depict a sharp contrast in the material distribution across spatial boundaries, the composition of the FGMs varies consistently in the spatial domain.

Most of the popular techniques for the representation of FGM are based on spatial distribution, and the subsequent material distribution in space. The existing process planning techniques for SFF are based on the trivial assumption of material homogeneity that deals only with the geometrical aspects of the part. However, for FGM, in addition to the geometry of the part, the composition of constituent material needs to be addressed. The reported methods that address issues pertaining to the actual process implementation [**12–14**, **17**] are not very flexible and require a special set-up. The method proposed by Liu *et al.* [**18**] depends on an exhaustive approach of accessing the individual points of delivery, and is applicable to the systems for which the material storage and delivery are connected by a near-zero-length conduit. The method suggested by Kumar *et al.* is based on the decomposition of solids owing to the regions of homogeneous composition; however, the method is applicable to heterogeneous solids and may not be applicable to a large class of FGM parts. Other methods suggested by Anping *et al.*, Zhou *et al.*, and Siu *et al.* assume a very simple material distribution model and hence are applicable to a smaller class of FGM.

The mathematical model of FGM is based on a continuous variation in the composition of the material at an infinitesimal order; however, owing to the limitation of the experimental set-up, the infinitesimal order is not possible, and the delivery of the material takes place for a non-infinitesimal amount. The dimensions of the molten pool are finite. Also, the smoothness of the deposition surface depends on the extent of overlap between the deposited

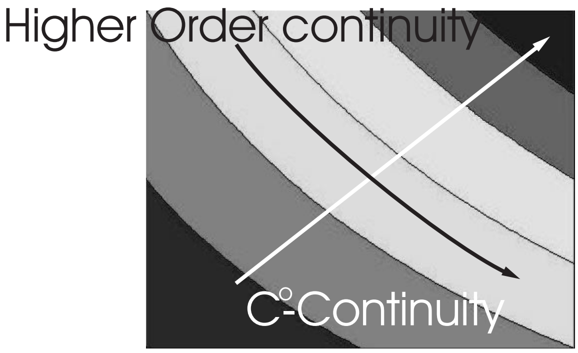

Fig. 2 Order of continuity along tangential and radial directions for FGM

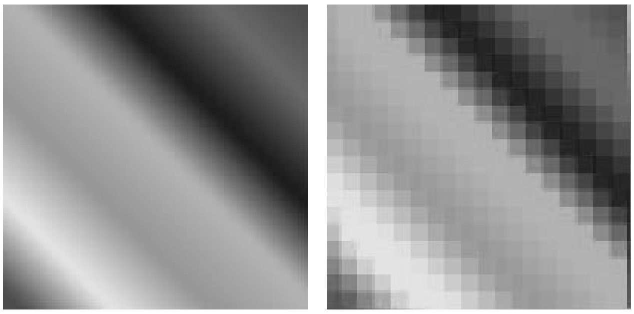

(a) Original Distribution of Material in FGM

(b) Sampled and Quantized material distribution in the FGM

Fig. 3 Sampling and quantization of FGM

beads. Another advantage that can be attributed to the overlap of beads is the remelting and mixing of material, thus allowing a better and near-net desired gradience of the material composition. The path spacing for deposition is the fraction of the actual bead/width so as to allow overlap between the beads.

Assuming that the composition of metal powder is homogeneous and is distributed evenly when delivered at a given spot, smooth variation in the material composition is possible only along the tangential direction of path-curves; the same is not possible along the normal direction. As shown in Fig. 2, control of the material composition is limited along the normal direction of the curves. A high-order continuity of material variation is sustained along the tangential direction of the tool path, whereas the nature of variation along the normal direction is limited and can be classified as C^0. Also, the minimum resolution of composition variation along the normal direction is limited by the size of the molten pool. This phenomenon suggests that a sampling and quantization-based approach can be adopted for the representation of the FGM. One of the advantages associated with the sampled representation of the part includes a limited amount of memory requirement for information storage. The memory requirement for information storage increases along with that of the order of material resolution.

Similarly to pixel and voxel-based quantization for image processing and computer graphics, respectively, to define the term '*maxel*': a maxel corresponds to the quantized material composition attributed to a sampled three-dimensional volume. The assignment of material attributes to the quantized volume is based on the composition averaged over the unit volume of each maxel. Maxel-based quantization is expressed as

$$f_s(x,y,z) = \sum_{p=1}^{p} \sum_{m=1}^{M} \sum_{n=1}^{N} f_{av}(m\Delta x, n\Delta y, p\Delta z) \times \delta(x - m\Delta x, y - n\Delta y, z - p\Delta z) \qquad (1)$$

where Δx, Δy, and Δz correspond to the size of the molten pool and hence the order of the sampling. For every layer, the variation along the z axis is ignored. The f_{av} is the composition averaged over one maxel area such that

$$f_{av}(x, y, z) = \frac{1}{\Delta x \Delta y} \int_{x-\Delta x/2}^{x+\Delta x/2} \int_{y-\Delta y/2}^{y+\Delta y/2} f(x,y,z)\mathrm{d}x\mathrm{d}y \qquad (2)$$

Note that the quantization scheme suggested in equation (2) ignores the variation of the material composition along the z direction. Figure 3 shows a sampled and quantized transformation model of an FGM. The figure is obtained by sampling the FGM over a distance of a molten poolwidth.

As described earlier the method used in these experiments for the material deposition employs laser-based metal deposition. Metal, which is added in the form of a powder stream, can be mixed, on the fly, to the desired composition. Owing to the finite size of the molten pool and the subsequent width of the deposition, the set of curves that comprise the tool path is a set of points P such that $P \in S$, where S is the set of points that constitutes the solid.

Another set of parameters that must be taken into account during the process planning includes the length of conduits and pipes that carry the stream of metal powder. Suffcient time must be allowed until the composition of the metal powder becomes homogeneous and the rate of flow is consistent. Therefore, the geometry of the path should be such that it follows the direction of least gradience of the composition. For certain regions, a smooth variation of composition may allow fabrication of the part by a coordinated control of electric drives. The same may not be possible for other regions where change in the composition of material is discontinuous. A shift of regions and discontinuity in metal deposition necessitates sufficient time to discharge the metal already present in the conduits and before another set of materials or composition becomes stable. Another factor associated with material variation is that material composition requires a change in the settings of the drives for the powder feeder and spatial movement. Therefore, the path planning method can address the following list of factors:

(a) the path along the direction of minimum descent of the composition variation;
(b) determination of the time required before delivery of the desired composition of material becomes uniform;
(c) the time before excess material is removed when shifting from one region to another;
(d) the geometric and the material parameters to be represented by a finite amount of data;
(e) the distance between the path segments taking into account the geometry corresponding to the size of the molten pool and the allowable overlap between the depositions.

2.1 Path planning approaches

The first step towards fabrication of the part by SFF is to slice the computer model of a solid into a set of layers. The next step is to generate a path for each layer. The path-planning technique for fabricating FGM must take into account the requirements for geometry as well as the material composition. The existing approaches of path planning are based on the trivial assumption of material homogeneity. This imposes the requirement of path planning for FGM to be viewed from an entirely different point of view.

The existing strategies for path generation may be classified into evolving curves, which include the zigzag and contour types, spirals, and space-filling curves [**9**, **20**, **21**]. The same idea may be extended to path planning for FGM with certain modifications. To define the iso-composition contour, which is widely used for the implementation of the process: the iso-composition contour corresponds to a two-dimensional curve that connects points with a similar composition. Figure 4(a) shows an FGM solid, Fig. 4(b) is the sliced model and the subsequent iso-composition contours derived for each of the fields. Figure 4(c) depicts a set of iso-composition contours derived from a two-dimensional field arranged in the order of variation of the composition.

Contrary to the popular methods of representation that are based on the subdivision of volume of the original solid into a set of subvolumes and attributing the material to each subvolume, the current authors propose an algorithm based on the representation of the solid by spatial curves corresponding to the torch path and attributing the material properties to each curve. The algorithm may be described as:

Step 1. Slice the solid.
Step 2. For each slice, segment the area of the slice based on the boundaries that depict a sharp variation in the metal composition.
Step 3. For every region connect the points of similar composition to generate isocomposition contours. The distance between the isocomposition contours is governed by the minimum allowable distance in deposition.
Step 4. Arrange the order of build for each curve based on the minimum variation of the material composition.
Step 5. When the distance between two isocomposition contours is more than the allowable distance, generate the intermediate curves by interpolation.

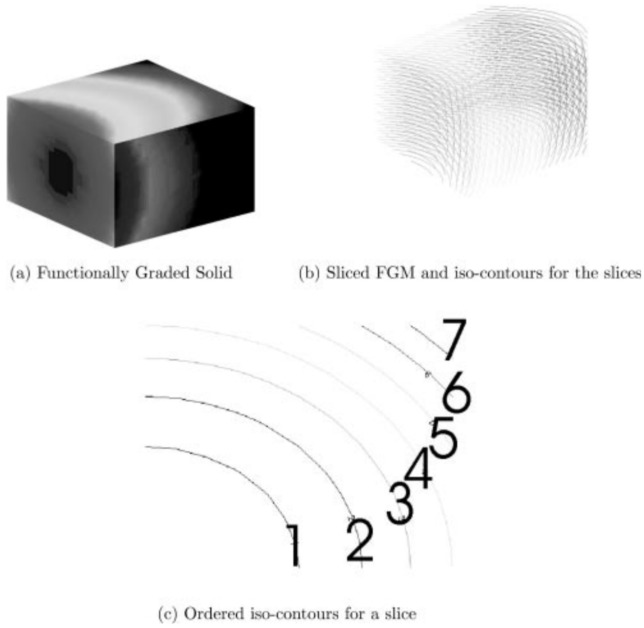

Fig. 4 Slicing and derivation of isocomposition contours for an FGM solid

Attributing the order of the build in step 4 minimizes material wastage. In a given region, a shift from one isocomposition contour to another may require a small variation in the material composition. The time required for the discharge of extra material, and the wait time before composition of material becomes uniform and consistent is reduced just by a small alteration in the state of the feeder drives. Step 5 is required for the FGMs that have a spatially non-uniform distribution of material.

3 PROCESS PLANNING MODEL FOR FABRICATING FUNCTIONALLY GRADED MATERIAL PARTS

The desired composition of a part made of functionally graded material is governed by the desired function of the part. While certain regions of the part have a non-varying material composition, other regions have a varying multimaterial composition. Based on the distribution of material composition, the composition is represented by a vector field such that a vector corresponding to the composition of material is attributed to every point in the space as it changes from point to point.

FGM material can be expressed by the material vector-space of order m where each coordinate corresponds to a constituent material. The geometric topology of the FGM is expressed by the underlying manifold $M^3$of the Euclidian space of order 3 corresponding to the x, y, and z coordinates. The concept of manifold-and-material space, in essence, captures the intent of spatial-and-material composition continuity. The projections of the manifold-and-material function in the material space along the individual coordinates provide the input for process implementation.

The approach based on establishing a one-to-one correspondence between the spatial regions inside the solid and the composition of the constituent materials result in an undesirable C^0 continuity. Introducing time as a parameter so as to express the process model as phase spaces, models the process as a high-dimensional manifold with a vector field indicating how the system changes over time. The inclusion of time to express the spatial motion of the metal deposition head-and-material composition as a function of time ensures a higher order of continuity across the part domain. Also, the time derivative of the spatial function determines the velocity or the input for the spatial manipulator. Similarly, the arrangement of isocomposition curves in the order of composition variation allows for continuity in the state of the drives that control the delivery of material. For all practical purposes, the manifold M^3 is a topological manifold. A manifold χ is a topological manifold if:

(a) χ is locally Euclidean with constant local dimension 3 in the present case;
(b) χ is second countable;
(c) χ is a Hausdorff space.

The composition vector field is a vector each of whose components is a scalar field; that is, a function of spatial and time components expressed as

$$M(x, y, z, t) = m_1(x, y, z, t)\hat{\mathbf{e}}_1 + m_2(x, y, z, t)\hat{\mathbf{e}}_2 + m_3(x, y, z, t)\hat{\mathbf{e}}_3 + \cdots + m_n(x, y, z, t)\hat{\mathbf{e}}_n \quad (3)$$

where M represents the vector field, x, y, z correspond to the spatial coordinates of the part, t is time and m_1, $m_2, \ldots$, represent the spatial function of the part material fraction in the composition at the point of consideration.

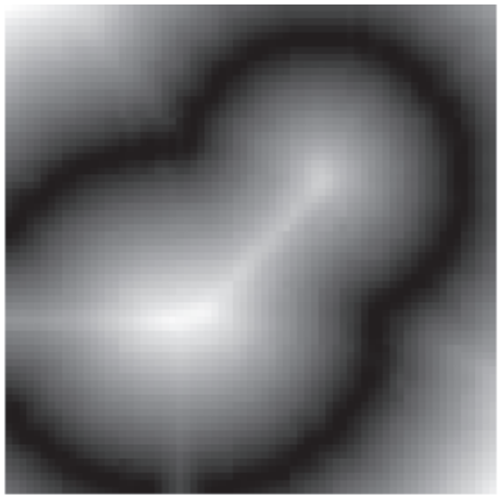

(a) Original Distribution of Material in FGM

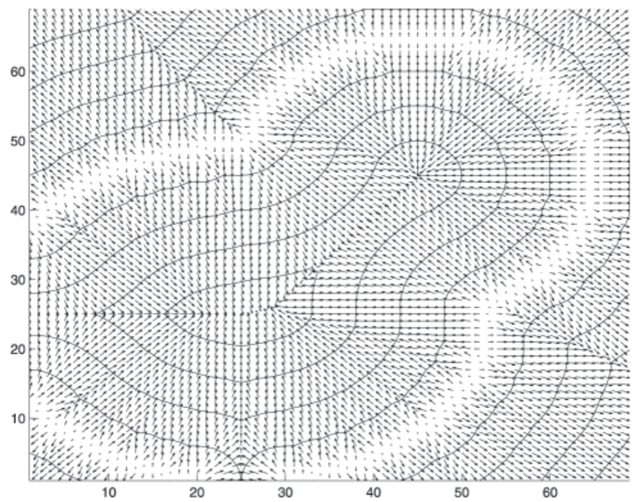

(b) The Gradient of material distribution in the FGM

Fig. 5 Gradient of material distribution in the FGM

One of the conditions that must be satisfied is that the material fraction at a given point must add to unity

$$\sum_{i=0}^{n} m_i(x, y, z, t) = 1 \quad (4)$$

One important class of vector field that is derived from the computer model is the gradient of a scalar field for the material distribution. If f is a scalar field, its gradient, ∇f is a vector field, namely

$$\nabla f = \frac{\partial f}{\partial x}\hat{\boldsymbol{\imath}} + \frac{\partial f}{\partial y}\hat{\boldsymbol{\jmath}} + \frac{\partial f}{\partial z}\hat{\boldsymbol{k}} \quad (5)$$

The vector field thus obtained (Fig. 5(b)) as the gradient of the material composition provides input for the process planning. In order to be able to use the data for process implementation, it is important to acquire different components of the vector field. The desired components of the field include curves formed by connecting all the points having a similar composition and the curves that are directed along the direction of gradience, that is, the divergence of the vector field.

'Isocomposition contours' – these refer to curves that are obtained by connecting the maxels of a layer that have a similar composition. The set of composition contours thus obtained comprises the metal deposition head path. The isocomposition contours in essence refer to the equipotential surfaces in the three-dimensional material composition field. The curves representing the divergence of the field provide the direction of propagation of the isocomposition contours. To summarize the idea, the two foremost essential components that need to be derived are:

(a) the gradient using the divergence operator;
(b) the equipotential contours.

Using the fluid analogy of a field, Helmholtz–Hodge decomposition can be used such that the field inside a region is given by

$$\mathbf{\Phi} = \nabla u + \nabla\times\mathbf{v} + \mathbf{h} \tag{6}$$

where u is a scalar potential field, $\mathbf{v}$ is a vector potential field, and $\mathbf{h}$ is a harmonic vector field such that following conditions are satisfied by the individual components

$$\nabla \times (\nabla u) = 0 \tag{7}$$

$$\nabla(\nabla \times \mathbf{v}) = 0 \tag{8}$$

$$\nabla\mathbf{h} = 0 \tag{9}$$

$$\nabla \times \mathbf{h} = 0 \tag{10}$$

One of the essential parameters included in the representation is time. A time derivative of the values obtained provides inputs for the system drives, including the drives for spatial manipulators and metal-powder feeders. For a feasible representation of the solid, the point sets used to model it must be described by a finite amount of data. The actual process implementation is concerned only with the set of points visited by the metal deposition head during the deposition. The set of points may be described by piecewise continuous linear- or higher-order functions. Another set of functions pertaining to the material composition can be attributed to the path-curve functions. The common parameter between the two functions is time. The following sections elaborate the methods used to implement the above requirements in detail. The maxel representation of the FGMs allows the application of the image processing algorithms based on convolution to derive the inputs for the process implementation. The following subsections elaborate the approach used to identify the process inputs by the processing of the maxel data representation of the solid.

3.1 Segmentation of the slice area for contour generation

A trivial approach based on the existence of a uniform material composition across the geometry of the part may not be applicable to parts that depict a sharp variation in gradience across spatial boundaries. A smooth variation of the field can be attributed to various subregions in the material field, and a suitable scheme can be used for path-planning in the region. However, the identification of subregions is based on the determination of the regions that exhibit a sharp variation or abrupt variation, in essence the boundary of the subregions. The authors employ edge detection techniques for the determination of boundary contours. The edge detection for a field is based on the determination of the second-order gradient using the Laplacian transform of the material scalar field given by the following expression

$$\nabla^2 M(x,\ y,\ z,\ t) \tag{11}$$

The Laplacian operation expands to

$$\begin{aligned}\nabla^2 M(x,y,z,t) &= \left(\frac{\partial^2 m_1(x,y,z,t)}{\partial x^2} + \frac{\partial^2 m_1(x,y,z,t)}{\partial y^2} + \frac{\partial^2 m_1(x,y,z,t)}{\partial z^2}\right)\hat{e}_1 \\ &\quad + \left(\frac{\partial^2 m_2(x,y,z,t)}{\partial x^2} + \frac{\partial^2 m_2(x,y,z,t)}{\partial y^2} + \frac{\partial^2 m_2(x,y,z,t)}{\partial z^2}\right)\hat{e}_2 \\ &\quad + \dots \\ &\quad + \left(\frac{\partial^2 m_n(x,y,z,t)}{\partial x^2} + \frac{\partial^2 m_n(x,y,z,t)}{\partial y^2} + \frac{\partial^2 m_n(x,y,z,t)}{\partial z^2}\right)\hat{e}_n\end{aligned} \tag{12}$$

The Laplacian operator over the sampled three-dimensional field is implemented by summing the components along individual directions expressed as

$$\begin{aligned}\nabla^2 m_i(x,y,z,t) = {} & m_i(x+1,y,z,t) + m_i(x-1,y,z,t) \\ & + m_i(x,y+1,z,t) + m_i(x,y-1,z,t) \\ & + m_i(x,y,z+1,t) + m_i(x,y,z-1,t) \\ & - 6m_i(x,y,z,t)\end{aligned} \tag{13}$$

However, the above technique is implemented for individual layers; therefore, the implementation is governed by an elimination of the terms corresponding to the distribution of material along the z axis, as given below

$$\begin{aligned}\nabla^2 m_i(x,y,t) = {} & m_i(x+1,y,t) + m_i(x-1,y,t) \\ & + m_i(x,y+1,t) + m_i(x,y-1,t) \\ & - 4m_i(x,y,t)\end{aligned} \tag{14}$$

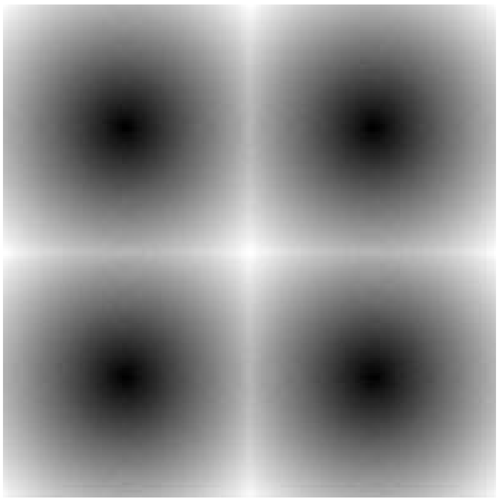

(a) Original Distribution of Material in FGM

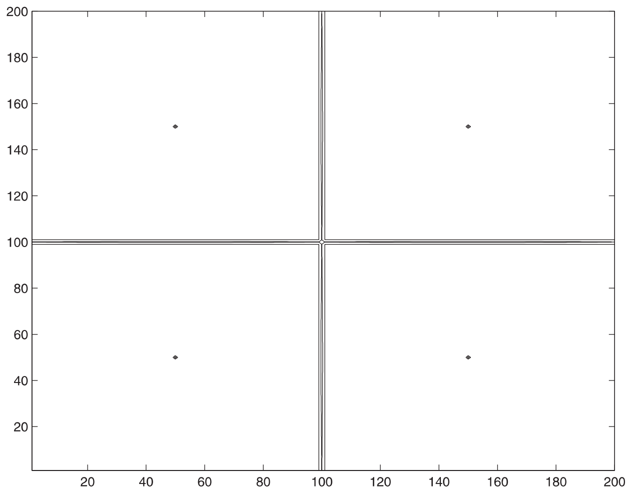

(b) Division of the FGM into subregion

Fig. 6 Division of FGM into subregions

A more detailed account of the determination of the Laplacian operator in a two-dimensional field is elaborated in [**22**].

Figure 6(a) shows the material field of an FGM. Figure 6(b) shows the subsequent segmentation of the field into subregions, based on the Laplacian operator.

3.2 Determination of the curl and divergence components using fluid analogy for FGM

The isopotential component of the field, as described earlier, corresponds to the isocomposition contour. This is identified using the nearest neighbour criterion. Starting from any maxel, the composition of the nearest seven neighbours is compared. The maxel under investigation is located on the

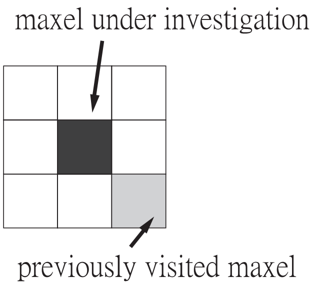

Fig. 7 Nine-maxel window for the generation of an isocomposition contour

centre of the nine-maxel window (Fig. 7). Whereas one of the maxels corresponding to the previsited maxel is ignored, the maxel having a composition similar to that being investigated is attributed to the list of maxels that generate the isocomposition contours.

The determination of the gradient field is based on attributing the composition gradient vector to every maxel. The composition gradient vector is the difference in the composition between adjacent maxels. The difference between adjacent maxels is determined along the maxel direction for the horizontal and vertical components of the gradient vector. The divergence is based on the cubic interpolation through the *maxels* such that the slope of the gradient curve is directed along the gradient vector at the given maxel location.

Figure 8 elaborates a material field and the corresponding derived inputs, namely isopotential curves (Fig. 8(b)) and gradient (Fig. 8(c)). Figure shows the curves corresponding to the gradient of the field. Figure shows the isocomposition contour curves determined by connecting the maxels with similar composition.

A linear increment in specifying the material composition for the generation of isocomposition curves may suffce for most of the FGM parts. The isocomposition curves thus generated are parallel and equidistant; however, the approach needs a modification if the distribution of the composition is non-linear. To determine the distribution of isocomposition curves, the authors use the principle of histogram equalization borrowed from image processing. The histogram equalization depicts the distribution of the composition as a function of area. The area here refers to the number of units of maxel area. The unit area is governed by the beadwidth.

3.3 Adaptive isocontour generation

Adaptive isocomposition curve generation, also referred to as morphing [**23**], is based on the

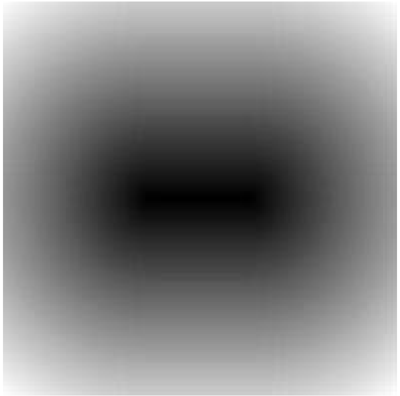

(a) Original Functionally Graded Solid

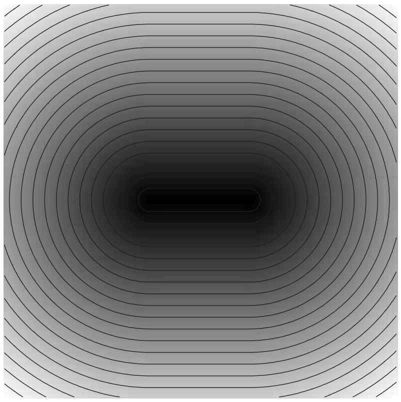

(b) Iso-potential (-composition) component

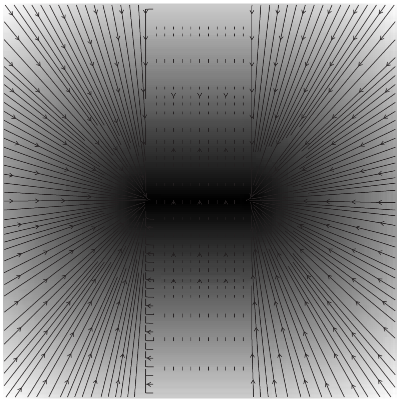

(c) Composition divergence

Fig. 8 Derivation of different components for process planning

wave-front propagation model. A propagation curve is given by

$$r_{\text{offset}}(u) = r_{\text{original}}(u) + \mathbf{n}(u)d \tag{15}$$

where d is the offset distance, $\mathbf{n}$ is the vector directed along the direction of offset, $r_{\text{offset}}(u)$ and $r_{\text{original}}(u)$ correspond to the offset and the original curves respectively.

The steps for the contour generation are:

Step 1. Determine the isocontours of the area.
Step 2. Determine the isocontour with the minimum area.
Step 3. Offset the isocontour by a distance equal to the allowable distance between two beads.
Step 4. Find out the composition of all the points on the offset curve.
Step 5. Determine the point having maximum variation of composition with respect to the initial isocontour and connect all the points having similar composition in order to find the next isocontour.
Step 6. Repeat steps 3 to 5 unless the end of the region is reached.

The regions where the distance between adjacent isocontours is more than the allowable distance, i.e. the beadwidth, generate the contour and assign the composition to it based on interpolation. Let D_r be the minimum distance between two iso-composition curves and w be the allowable distance between two path segments. If $D_r \geqslant w$, then a generation of the intermediate path segment is required. Let χ_{ip} correspond to the composition of the ith material in the pth contour. The number of intermediate segments required is $L = [D_r/(w) - 1]$ where [] corresponds to the greatest integer function. The composition of the qth segment such that $1 \leqslant p \leqslant L$ is given by

$$\chi_{\text{ip}} = I(r)\chi_{\text{i1}} + I(L - r)\chi_{\text{iL}} \tag{16}$$

$I()$ is a suitable interpolation function. The function I() depends on the divergence of the material field. The divergence of the field is used to obtain the curves corresponding to the stream function of the field. For simple fields, the stream function is simpler; whereas, for complex fields that are based on frequent variation of material field over the space, the stream function and hence the interpolation function may be complex. Depending on the desired composition and accuracy of the composition, function $I()$ may be linear or non-linear. The same formula holds for two isocomposition contours that are not parallel; however, the distance between two isocomposition contour curves changes; therefore, the method requires a modification. Two curves are divided, based on the incremental distance of the allowable width between two path curves. The procedure for the generation of intermediate curves is repeated for each set of curves.

Figure 9(a) shows a set of non-uniformly distributed isocomposition contours and the interpolated curve for a slice. The composition of the isocontour curves for two materials varies from 60:40 to 70:30. Figures 9(b) and (c) show the variation in the composition of the interpolated isocomposition curve with respect to the desired composition. The deviation in the composition is negligible. A unique composition can be attributed to the interpolated isocomposition curve. However, for the critical parts, an interpolated curve may be decomposed into a set of curves, and a suitable uniform composition can be attributed to each segment of the decomposed curve.

4 DETERMINATION OF THE TIME FOR POWDER FLOW STABILITY

The time span for material discharge depends on the total distance from the point of emanation at the powder feeder and the delivery nozzle, and the speed at which the material moves. While the cross-sectional area of the conduits for individual metal powders is the same, the length may vary. Sufficient time must be allowed before the flow becomes stable. Another factor that plays an important role is the time required before sufficient mixing has taken place between individual constituents, and the delivery of composition has become stable. The time required for a particle p to travel from the point of origin to the point of delivery is expressed by

$$t_p = \frac{L_p}{v_p} \tag{17}$$

where L_p is the distance between the origin and the delivery point and v_p is the speed of the movement of the particles.

The total time required before the composition of the delivery of the material from the individual powder feeders reaches a stable rate is

$$t_{\max} = \max(t_1, t_2, \ldots, t_n) \tag{18}$$

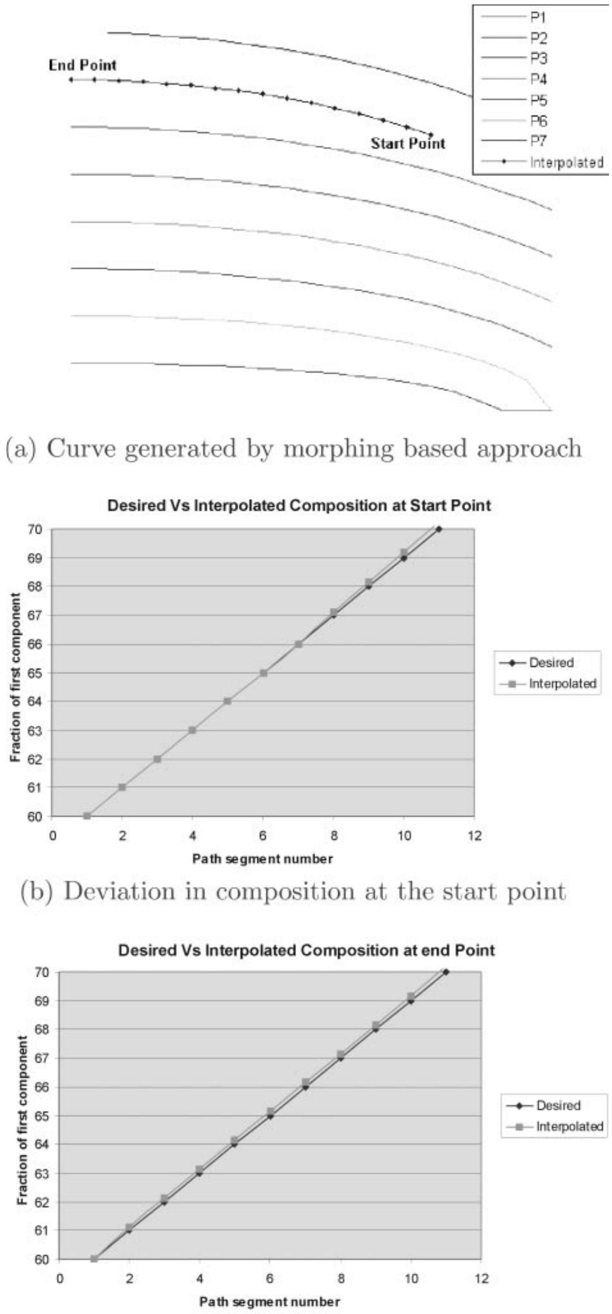

(a) Curve generated by morphing based approach

(b) Deviation in composition at the start point

(c) Deviation in composition at the end point

Fig. 9 Generation of the tool path by morphing

where t_i corresponds to the time for the ith metal powder stream. For practical purposes, the speed of the powder delivery for the individual components may be assumed to be the same; therefore, the total time before the delivery of the metal composition at the point of delivery becomes uniform is given by

$$t_{\max} + \frac{L_{\mathrm{f}}}{v} \tag{19}$$

where L_{f} is the length of the conduit that connects the meeting point of all individual carrier conduits to the delivery nozzle.

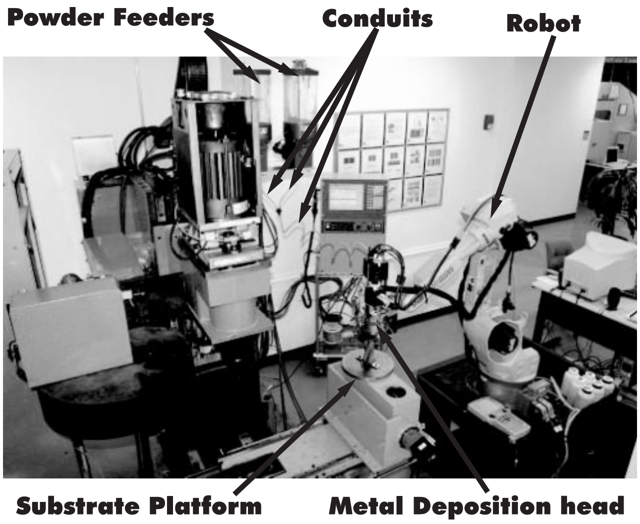

Fig. 10 MultiFab system used for the fabrication of FGM

Therefore, the expression for the overall time for the delivery of the powder is given by

$$t_{\text{total}} = \frac{\max(L_1, L_2, \ldots, L_n)}{v} + \frac{L_f}{v} \tag{20}$$

where L_i corresponds to the length of the ith metal powder carrier conduit and v is the speed of the powders; in essence, the carrier gas.

5 PROCESS IMPLEMENTATION AND THE EXPERIMENTAL SETUP

The Research Center for Advanced Manufacturing, at SMU Dallas, Texas is developing a 'MultiFab' machine that integrates various deposition and machining techniques on one PC-controlled set-up for fabrication of the part. One of the features of the machine includes the ability to fabricate FGM parts. Figure 10 shows the MultiFab used for laser-based deposition for the fabrication of FGM parts. Powder feeders store the powder. A computer-based controller mounted on the powder feeder controls the delivery rate. The metal deposition head is mounted on a six-axis robot, and the substrate is mounted on a platform that is manipulated in the space. The coordinated motion of the robot and the substrate fabricate to the desired geometry. A feed-forward-based approach allows the coordination of motion of the substrate, powder delivery head, and laser power. The time taken for the deposition head to travel a designated path segment is estimated. Also, the time required for the discharge of extra metal powder, and the time before the composition of the powder becomes uniform is estimated beforehand. The sequence of operation is set and offloaded in the form of a code to the computer that communicates with the MultiFab machine. The time assignment for a path segment k is elaborated in Table 1.

A computer-based controller for the powder feeders controls the material composition. Inputs for the process implementation are: the position, velocity of the deposition head, and corresponding material composition. The position and the material composition are coupled with time as a common parameter. In order to have a uniform deposition, the velocity and material delivery must be compatible. For example, the volume delivery must be such that the volume of the material discharge is constant over time, while there may be a variation in the individual components of the motion such as v_x, v_y, v_z. The overall magnitude of velocity must be a constant, expressed as

$$\sqrt{v_x^2 + v_y^2 + v_z^2} = V_c \tag{21}$$

Similarly, the rate of addition of material should be constant such that

$$\sum_{i=0}^{n} \dot{m}_i = C \tag{22}$$

where $\dot{m}_i$ corresponds to the rate of change of the ith material constituent, and n is the maximum number of material constituents. The coding format of the output for the process implementation is given by

$$t_i \; v_x, \, v_y, \, v_z \; \dot{m}_i, \, \dot{m}_2, \ldots, \dot{m}_n, \, \mathit{LaserStatus}$$

6 RESULTS

A Matlab-based code was developed for process planning. The input for the code is a solid model that stores spatial geometry of the part and the desired material distribution function representing the material composition field. Other inputs include the beadwidth, extent of overlap, and layer thickness.

The process planning starts with the voxel model of the solid. Next, the desired material field is overlapped onto the voxel model to generate the maxel distribution. Figure 11 shows a solid model, the slices of the voxel model derived from the solid model, and the overlap of material field on the voxel model for the solid.

Next, the edge detection identifies the subregions in the part. This is then sliced by a set of parallel planes and the intersection of the planes with respect to the subregions provides a set of curves for each layer. Connecting the points with similar composition generates the isocomposition contours,

Table 1 Time assignment for a path segment k

Time	$\overset{k}{\leftarrow} t_1$	$\overset{k}{\leftarrow} t_2$	$\overset{k}{\leftarrow} t_3$	$\overset{k}{\leftarrow} t_4$
Path	Starting point	Starting point	$\int_{t_3}^{t_4} \overrightarrow{\mathbf{V_1}}\,\mathrm{d}t$	End point
Velocity	$\mathbf{v} = 0$	$\mathbf{v} = 0$	$\mathbf{v} = \mathbf{v_k}$	$\mathbf{v} = 0$
Material delivery	No addition, material from previous region discharged	Material added in new composition till uniform flow	Uniform flow of the composition χ_k	No addition till all material is discharged
Laser status	Off	Off	On	Off

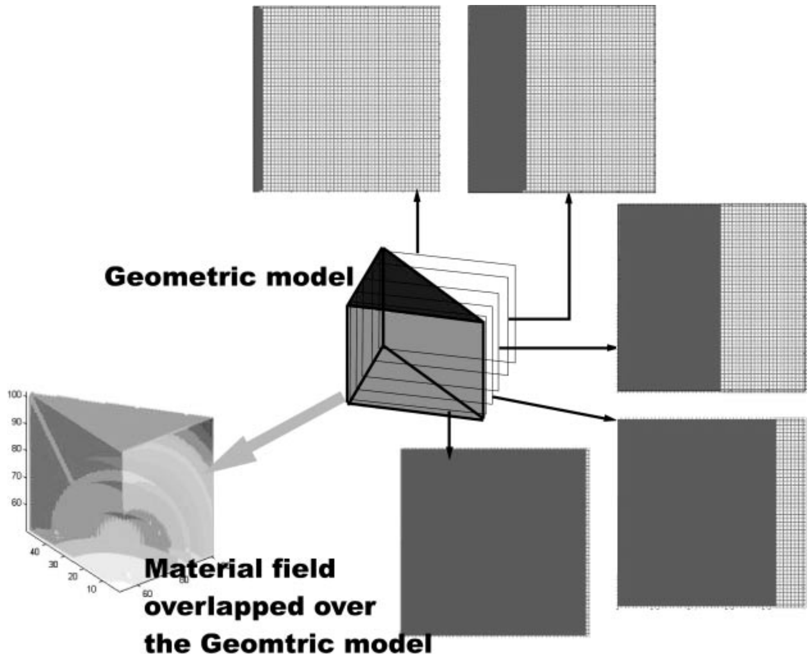

Fig. 11 Solid model, voxel model for the solid model and the overlap of the material field on the voxel model. (Note that for each slice, the grid region depicts the void, whereas the solid region depicts the voxel element.)

and the intermediate path segments are generated by interpolation, as explained earlier.

One of the FGM functional components fabricated using the laser-based deposition is the pin for friction stir welding (FSW). The FSW process utilizes local friction heating to produce continuous solid-state seams, and joins materials by plasticizing and then consolidating the material around the joint line. The process is implemented by piercing a hole at the start of the joint with a rotating pin. The pin continues to rotate and moves forward in the direction of welding. As the pin proceeds, the friction heats the surrounding material and rapidly produces a plasticized zone around the pin. Pressure provided by the pin forces plasticized material to the rear of the pin where it consolidates and cools to form a bond. The computer model of the tool is shown in Fig. 12. An FSW tool and a coupon prepared by the FSW are shown in Fig. 13.

The desired properties of the pin include a ductile and smooth interior, and a wear and heat-resistant exterior. During the process large thermomechanical stresses are generated. Therefore, a sharp contrast in the material composition is highly undesirable. A smooth gradience of the material composition

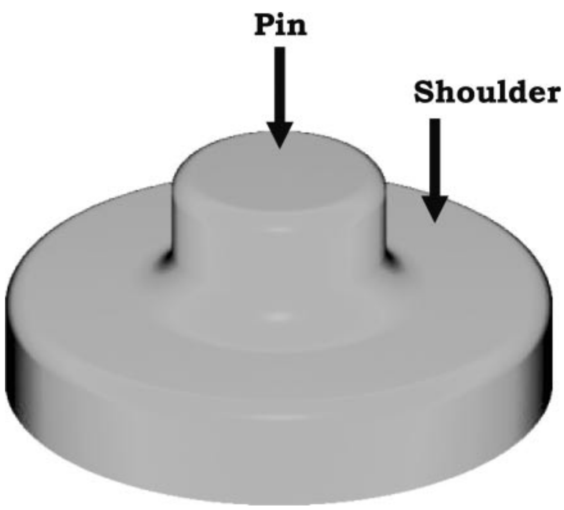

Fig. 12 Computer solid model of the FSW tool

from the core to the external surface avoids the development of high stresses. LBDMD is used to fabricate the tools for FSW [**24**].

The laser-based direct deposition is used to fabricate the tools for FSW. The material gradient varies from 100 per cent H13 to the composition of 50 per cent H13 and 50 per cent WC along the annular region of the tool to the external boundary of the solid.

Fig. 13 FSW tool and a coupon prepared using FSW friction stir welding

Figure 14(a) shows the desired distribution of the material whereas Fig. 14(b) describes the distribution based on the extraction of isocontours. Figure 14(c) is the path for the shoulder and Fig. 14(d) shows the path for the overall tool and the pin.

Figure 15 shows the actual tool fabricated using the process and the subsequent distribution of material obtained by mixing of the powders. As seen in Fig. 15, the melting allows mixing of the molten material so as to have a smooth gradient of the material distribution.

7 CONCLUSIONS AND FUTURE WORK

A process-planning approach for the fabrication of the FGM parts has been described. The method is based primarily on a fluid analogy of the material field. Using a framework of geometric reasoning, different components of the material field are determined and used for process planning. The algorithm is implemented using a Matlab-based code. For a given FGM part, the path is generated and described. A study of the microstructure and the comparison suggest that the approach is effective for the fabrication of functionally graded materials.

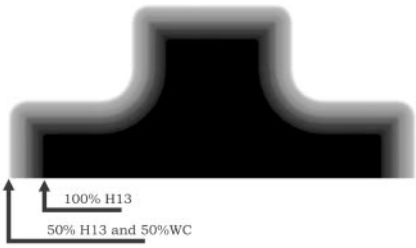

(a) Desired metal distribution

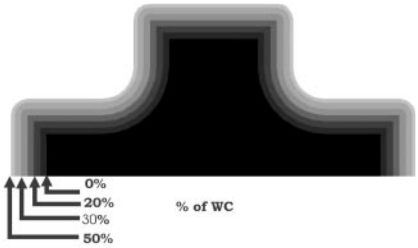

(b) Computer Generated model and the distribution

(c) Tool Path for the shoulder

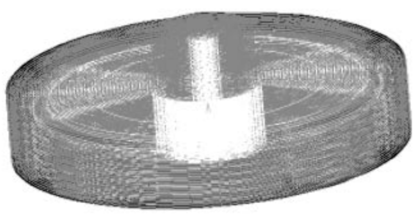

(d) Path for the complete tool (tool and shoulder)

Fig. 14 Computer modelling and tool-path generation

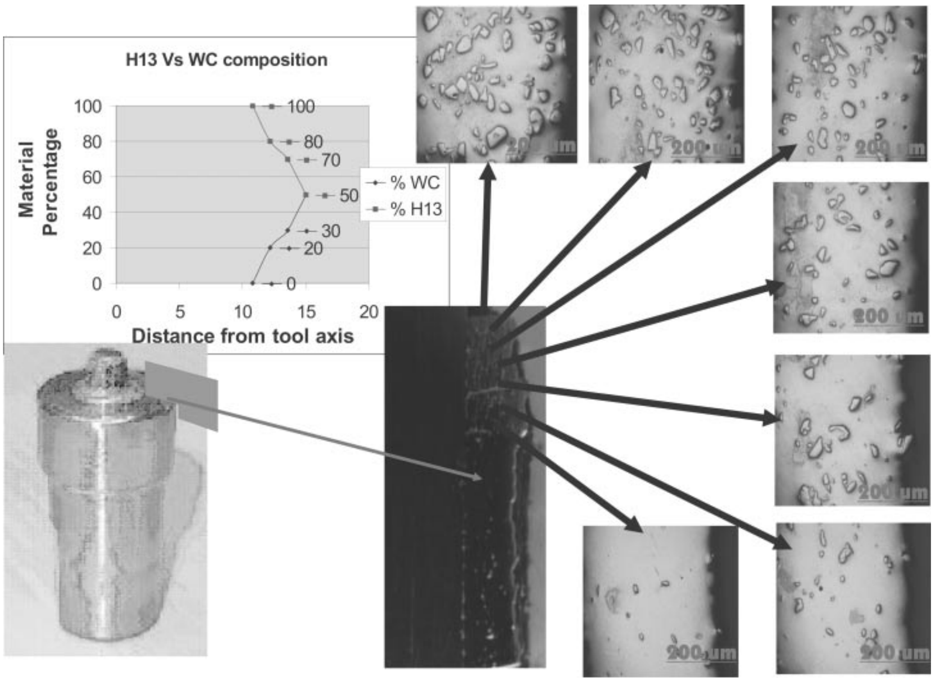

Fig. 15 Microstructure of the FSW tool and the material distribution

ACKNOWLEDGEMENTS

This work was financially supported by a THECB (Texas Higher Education Coordinating Board) Grant 003613-0016-2001 and an NSF (National Science Foundation) Grant DMI-0320663. The authors would like to acknowledge the help from Mr Michael Valant, Research Engineer, Research Center for Advanced Manufacturing.

REFERENCES

1 **Miyamoto, Y., Kaysser, W., Rabin, B., Kawasaki, A.,** and **Ford, R. G.** Functionally graded materials: design, processing and applications, Materials Technology Series, 5 October 1999.

2 **Ensz, M.** and **Griffith, M.** Critical issues for functionally graded material deposition by laser engineered net shaping LENS™. In Proceedings of the 2002 MPIF Laser Metal Deposition Conference, San Antonio, Texas, 2002, pp. 455–460.

3 **Griffith, M. L., Harwell, L. D., Romero, J. T., Schlienger, E., Atwood, C. L.,** and **Smugeresky, J. E.** Multi-material processing by LENS ™. In Proceedings of the 1997 Solid Freeform Fabrication Symposium, Austin, Texas, 1997, pp. 387–393.

4 **Pegna, J.** and **Sail, A.** CAD modeling of multi-modal structures for freeform fabrication. In Proceedings of the 1998 Solid Freeform Fabrication Symposium, Austin, Texas 1998.

5 **Kumar, V.** and **Dutta, D.** An approach to modeling multi-material objects. In Proceedings of the 1997 ACM Solid Modeling Conference, Atlanta, Georgia, 1997, pp. 336–345.

6 **Jackson, T. R., Liu, H., Patrikalakis, N. M., Sachs, E. M.,** and **Cima, M. J.** Modeling and designing functionally graded material components for fabrication with local composition control. *Mater. Des.*, 1999, **20**(2/3), 63–75.

7 **Biswas, A., Shapiro, V.,** and **Tsukanov, I.** Heterogeneous material modeling with distance fields. *Computer Aided Geometric Des.*, 2004, (21) 215–242.

8 **Jackson, T.** *Analysis of functionally graded material object representation methods.* PhD Thesis, Massachusetts Institute of Technology, Ocean Engineering Department, Cambridge, Massachusetts, 2000.

9 **Sarma, R.** An assessment of geometric methods in trajectory synthesis for shape creating manufacturing operations. *J. Mfg Syst.*, 2000, (19), 59–72.

10 **Kumar, V.** and **Dutta, D.** An approach to modeling and representation of heterogeneous objects. *J. Mech. Des.*, 1998, **120**(12), 659–667.

11 **Bhashyam, S., Shin, K. H.,** and **Dutta, D.** An integrated CAD system for design of heterogeneous objects. *Rapid Prototyping J.*, 2000, **6**(2), 119–135.

12 **Shin, K. H., Natu, H., Dutta, D.,** and **Mazumder, J.** A method for the design and fabrication of heterogeneous objects. *Mater. Desi.*, 2003, **24**, 339–353.

13 **Siu, Y. K.** and **Tan, S. T.** Slicing and contours generation for fabricating heterogeneous objects. In Proceedings of the Geometric Modeling and Processing – Theory and Application, 2002, pp. 219–225.

14 **Zhou, M. Y., Xi, J. T.,** and **Yan, J. Q.** Modeling and processing of functionally graded materials for rapid prototyping. *J. Mater. Processing Technol.*, 2004, **146**, 396–402.

15 **Patil, L., Dutta, D., Bhatt, A. D., Jurrens, K., Lyons, K., Pratt, M. J.,** and **Sriram, R. D.** Representation of hetergeneous objects in ISO 10303 (STEP). In ASME

International Mechanical Engineering Congress and Exposition, Orlando, Florida, 2000.

16 **Siu, Y. K.** and **Tan, S. T.** Source-based heterogeneous solid modeling. *Computer Aided Des.* 2002, **34**(1), 41–55.

17 **Anping, X.** and **Shaw, L. L.** Sff-oriented modeling and process planning of functionally graded materials using a novel equal distance offset approach. In The 15th Solid Freeform Fabrication Symposium, Austin, Texas, 2004, pp. 544–552.

18 **Liu, H., Patrikalakis, N. M., Sachs, E. M., Maekawa, T., Cho, W.,** and **Stratton, C. C.** A design and post-processing system for local composition control in solid freeform fabrication. In Proceedings of the 2004 NSF Design, Service and Manufacturing Grantees and Research Conference, Dallas, Texas, 2004.

19 **Kumar, V., Kulkarni, P.,** and **Dutta, D.** Adaptive slicing of heterogeneous solid models for layered manufacturing. *J. Mater. Processing and Mfg Sci.* 7.

20 **Dwivedi, R., Jandric, Z.,** and **Kovacevic, R.** Torch path planning for solid freeform fabrication based on welding. In Transactions of the North American Manufacturing Research Institution of SME, Vol XXXI, McMaster Univeristy, Hamilton, Canada, 2003, pp. 419–426.

21 **Dwivedi, R.** and **Kovacevic, R.** Automated torch path planning using polygon subdivision for solid freeform fabrication based on welding. *J. Mfg Syst., SME*, 2004, **23**(4), 278–291.

22 **Gonzalez, R. C.** and **Woods, R. E.** *Digital image processing*, 2nd edition, 2001 (Addison-Wesley Longman Publishing Co., Boston, USA).

23 **Dwivedi, R.** and **Kovacevic, R.** Morphing based approach for process planning for fabrication of geometries and the control of material composition. In the 15th Solid Freeform Fabrication Symposium, Austin, Texas, 2004, pp. 553–562.

24 **Ouyang, J., Mei, H., Valant, M.,** and **Kovacevic, R.** Application of laser cladding technique to the rapid manufacturing of tools for friction stir welding. In the 13th Solid Freeform Fabrication Symposium, Austin, Texas, 2002.